The Meteoritical Society

Meteoritics & Planetary Science 43, Nr 5, 823–828 (2008)
Abstract available online at http://meteoritics.org

Two distinct assemblages of high-pressure liquidus phases in shock veins of the Sixiangkou meteorite

Ming CHEN* and Xiande XIE

Guangzhou Institute of Geochemistry, Chinese Academy of Sciences, 510640 Guangzhou, China
*Corresponding author. E-mail: mchen@gig.ac.cn

(Received 04 June 2007; revision accepted 11 November 2007)

Abstract–Shock-produced complex veins, including earlier and later veins, are identified in the Sixiangkou L6 chondrite. The early vein is intersected by the late vein and consists of coarse-grained aggregates of ringwoodite, majorite, and lingunite, and fragments of olivine, pyroxene, plagioclase, metal, and troilite, as well as a fine-grained matrix of garnet, ringwoodite, metal, and troilite. The late vein mainly consists of a fine-grained matrix of garnet, magnesiowüstite, metal, and troilite, as well as a small amount of coarse-grained aggregates. The amount of fine-grained matrix suggests that the late vein was nearly completely melted, whereas the early vein underwent partial melting. Both fine-grained assemblages of garnet plus ringwoodite in the early vein and garnet plus magnesiowüstite in the late vein are liquidus phases crystallized from shock-induced melt. Based on our understanding of the liquidus assemblages, the late vein experienced a higher pressure and temperature than the early vein.

INTRODUCTION

Localized melting phenomena, such as shock veins, melt pockets, melt dikes, and metal-sulfide veins, have been observed in many chondritic meteorites, and attributed to disequilibrium shock effects (Fredriksson et al. 1963; Dodd and Jarosewich 1979; Rubin 1985; Stöffler et al. 1991). The high pressure and temperature history of some shocked L6 chondrites is confirmed by the occurrence of high-pressure minerals in the shock veins. These high-pressure minerals commonly occur as two assemblages, i.e., coarse-grained polycrystalline aggregates of ringwoodite, majorite, and lingunite (IMA2004-054) transformed from olivine, pyroxene, and plagioclase, respectively, as well as fine-grained liquidus phases crystallized from a shock-induced dense melt. Several typical liquidus assemblages have been reported in L6 chondrites. These are garnet plus magnesiowüstite in Sixiangkou (Chen et al. 1996), ringwoodite plus garnet in Roy (Xie et al. 2004), and akimotoite plus ringwoodite in Umbarger (Xie and Sharp 2004). Pressure and temperature conditions of the shock vein can be estimated according to the liquidus assemblages (Chen et al. 1996; Xie et al. 2004; Xie and Sharp 2004).

Most chondritic meteorites contain simple shock veins, i.e., veins forming at the same time and with no intersecting. Dodd et al. (1982) reported the first occurrence of complex veins in the Chantonnay L6 chondrite, in which an early vein containing abundant chondritic xenoliths is intersected by a late vein composed of a fine-grained matrix. However, high-pressure minerals were not investigated in the shock veins of Chantonnay. In this paper, we describe two distinct assemblages of high-pressure liquidus phases in the complex veins of the Sixiangkou meteorite.

SAMPLES AND METHODS

Polished thin sections containing shock veins and chondritic portions were made from the Sixiangkou meteorite. The shock veins and minerals were characterized using optical microscopy and a scanning electron microscope (SEM) in backscattered electron (BSE) mode. Chemical compositions of minerals were analyzed by a JEOL JXA-8100 electron microprobe (EMP) at 15 kV accelerating voltage and 10 nA beam current. Raman spectra of minerals were recorded with a Renishaw RM-2000 instrument to characterize their structures. A microscope was used to focus the excitation beam (Ar^+ laser, 514 nm line) to a 3 μm spot and to collect the Raman signal. Raman spectra were accumulated for 150 seconds.

COMPLEX VEINS

The Sixiangkou meteorite contains a number of shock veins intersecting the chondritic host. The widths of shock veins range from tens of μm to 10 mm. Some shock veins occur as simple veins mostly with thicknesses less than

Table 1. Compositions of minerals in the Sixiangkou meteorite by electron microprobe analyses (wt%).

	Chondritic portion			Early vein					Late vein	
				Coarse-grained aggregates			Liquidus phases		Liquidus phases	
	Olivine[a]	Pyroxene[b]	Plagioclase[c]	Ringwoodite	Majorite	Lingunite	Garnet	Ringwoodite	Garnet	Mw
SiO_2	38.0	54.8	65.0	38.0	54.8	64.9	53.3	38.6	52.2	1.1
MgO	38.2	27.7	<0.04	38.2	27.7	<0.04	26.9	37.4	28.0	34.9
CaO	0.04	0.95	2.1	0.04	0.95	2.1	1.1	0.09	2.2	n.d.
MnO	0.49	0.46		0.49	0.46	n.d.	0.52	0.34	0.34	n.d.
FeO	22.3	14.2	0.29	22.6	14.2	0.30	16.3	23.0	11.4	62.9
TiO_2	<0.04	0.17		n.d.	0.17	n.d.	0.28	<0.04	0.11	0.29
Al_2O_3	<0.04	0.15	21.0	n.d.	0.15	20.4	0.56	n.d.	3.7	n.d.
Cr_2O_3	0.04	0.13		0.04	0.13	n.d.	0.16	0.05	0.55	0.86
Na_2O	n.d.	0.04	9.6	n.d.	0.04	9.2	0.20	n.d.	0.99	n.d.
K_2O	n.d.	n.d.	0.98	n.d.	n.d.	1.5	n.d.	n.d.	n.d.	n.d.
Totals	99.07	98.60	98.97	99.37	98.60	98.40	99.32	99.48	99.49	100.05

Mw = magnesiowüstite; n.d. = not detected. Data of (a) and (b) are from Chen et al. (1996), and (c) from Gillet et al. (2000).

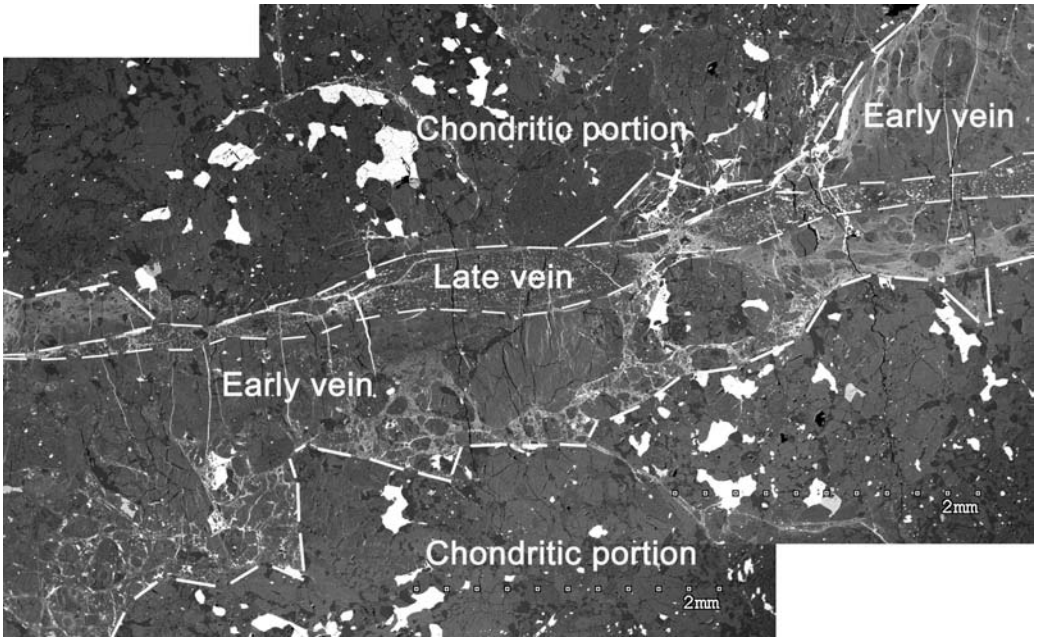

Fig. 1. Backscattered electron (BSE) image of polished thin section of the Sixiangkou meteorite. This image shows the occurrence of early vein, late vein, and chondritic portions. The early vein contains a number of coarse-grained fragments. The late vein mainly consists of fine-grained material. Note the jagged boundaries between the early vein and the chondritic portion.

200 μm. In addition to simple shock veins, we observe complex veins consisting of both the earlier vein and the later vein (Fig. 1). The widths of complex veins range from 200 μm to 10 mm.

Early Vein

The early veins make up the major portion of the complex veins. There are jagged boundaries between the veins and the host chondritic portion (Fig. 1). The vein consists of a number of mineral fragments and 30–40 percent fine-grained matrix.

The mineral fragments include both chondritic xenoliths (consisting of olivine, pyroxene, and plagioclase) and high-pressure polymorphs of silicates. More than 80 percent of the mineral fragments are high-pressure minerals. These high-pressure minerals occur as coarse-grained polycrystalline aggregates of ringwoodite, majorite, and lingunite transformed from olivine, low-Ca pyroxene, and plagioclase (or maskelynite), respectively. The smooth and round outlines of these aggregates are indicative of partial melting of previous olivine and pyroxene during shock-induced high pressures and temperatures. Electron microprobe analyses reveal that the compositions of ringwoodite, majorite, and lingunite are identical to olivine, pyroxene, and plagioclase in the chondritic portions (Table 1). Some large fragments olivine and pyroxene show local phase transformation along the rims of the grains (Fig. 2).

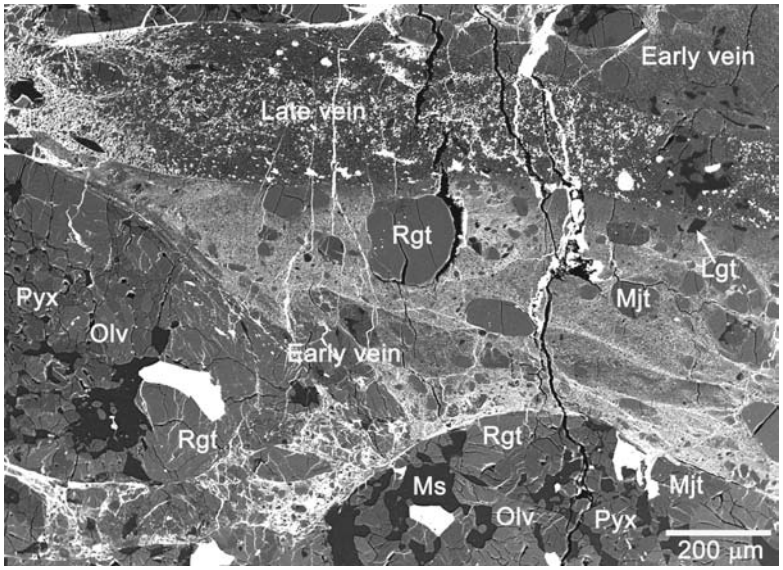

Fig. 2. BSE image showing knife-sharp boundaries between the late vein and the early vein. The early vein contains chondritic xenoliths or fragments consisting of olivine (Olv), pyroxene (Pyx) and maskelynite (Ms), as well as polycrystalline aggregates of ringwoodite (Rgt), majorite (Mjt), and lingunite (Lgt). Note that the coarse grained ringwoodite and majorite were enclosed in a fine-grained matrix.

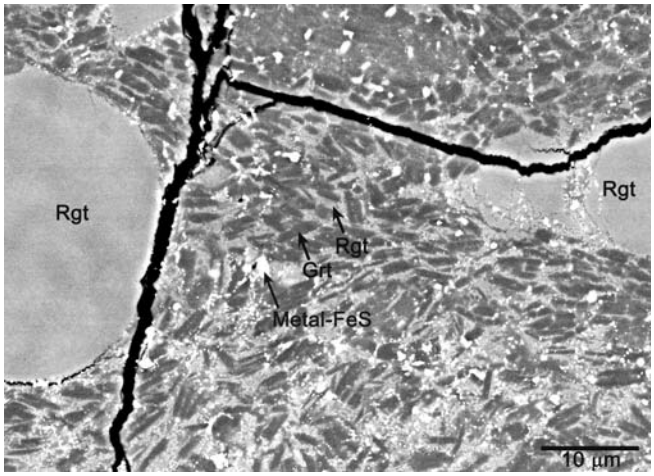

Fig. 3. BSE image of fine-grained matrix in the early vein showing columnar dendrites of garnet, granular ringwoodite, FeNi-metal, and troilite (FeS).

The fine-grained matrix consists of ringwoodite, garnet, Fe-Ni metal, and FeS sulfide (Fig. 3). Garnet occurs as columnar dendrites about 3 μm in length and 0.5 μm in width. Ringwoodite is granular and has grain sizes ranging from 50 to 100 nm. Figure 4 shows the Raman spectra of the matrix free of metal and troilite (Fig. 4), in which the bands at 586, 650, 930, and 1068 cm^{-1} can be assigned to garnet (Kimura et al. 2003), and the two strong bands at 799 and 842 cm^{-1} correspond to ringwoodite (McMillan and Akaogi 1987).

Broad beam analysis by electron microprobe reveals that the bulk composition of fine-grained matrix is similar to the bulk chondrite. The compositions of fine-grained ringwoodite in the matrix are the same as the coarse-grained aggregates of ringwoodite in the same vein and olivine in the chondritic host (Table 1). Garnet contains higher Al_2O_3 (0.56 wt%), CaO (1.1 wt%), and Na_2O (0.20 wt%) contents than the coarse-grained aggregate of majorite and low-Ca pyroxene (Table 1).

Late Vein

The thickness of the late vein is relatively thin and less than 500 μm in comparison with the thicker early vein (up to 10 mm). Most of the late vein is located within the early vein (Fig. 1); however, in places the late vein solely intersects the chondritic portion. Boundaries between the late vein and the early vein, or between the late vein and the chondritic portion, are sharp and occur as a knife-sharp contact (Fig. 2).

The late vein consists of fine-grained garnet, magnesiowüstite, Fe-Ni metal, and FeS (Fig. 5), and very small amounts of coarse-grained polycrystalline aggregates of ringwoodite and majorite. More than 90 percent of the vein is composed of the fine-grained material. Garnet in the matrix occurs as idiomorphic equant crystals ranging from 0.5 to 4 μm in diameter. Magnesiowüstite is granular or irregular in shape, with grain sizes up to 5 μm. It occurs in interstices within garnet. Magnesiowüstite less than 0.1 μm in size also occurs as inclusions in garnet.

The Raman spectrum of garnet displays several peaks at 586, 658, 802, 930, and 1068 cm^{-1} similar to garnet in the early vein (Fig. 6). Bulk compositions of the fine-grained matrix are similar to bulk chondrite (Chen et al. 1996). The garnet contains 2.2 wt% CaO, 3.7 wt% Al_2O_3, 0.55 wt% Cr_2O_3, and 0.99 wt% Na_2O. Magnesiowüstite contains 0.86 wt% Cr_2O_3.

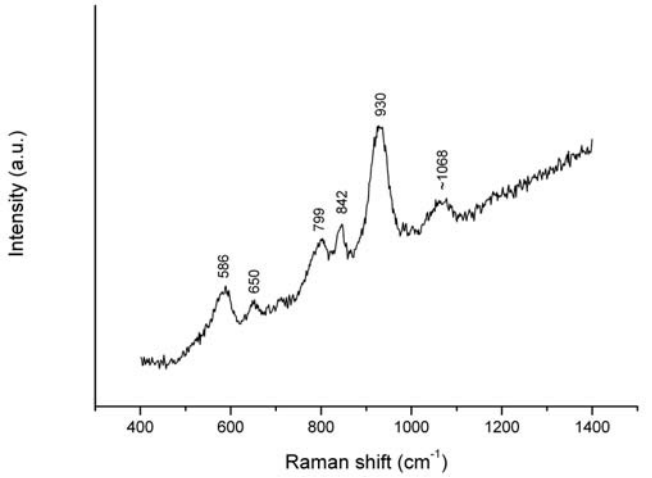

Fig. 4. Raman spectrum of fine-grained matrix free of metal and troilite in the early vein. The spectrum shows the bands from garnet (586, 650, 930, 1086 cm^{-1}) and ringwoodite (799, 842 cm^{-1}). a.u. = arbitrary unit.

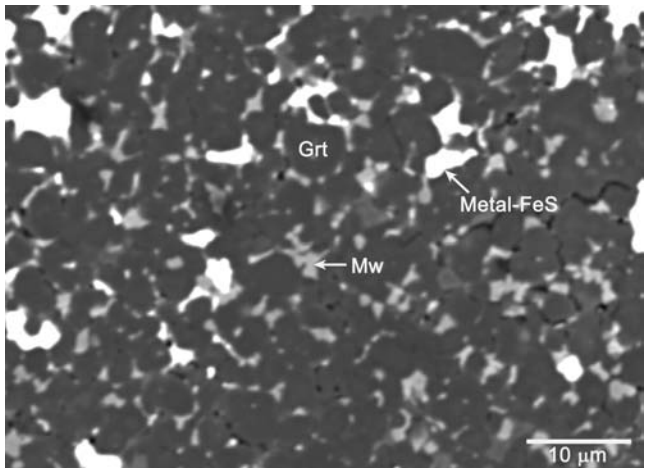

Fig. 5. BSE image of fine-grained matrix in the late vein showing equant garnet (Grt), granular to irregular magnesiowüstite (Mw), FeNi-metal, and troilite (FeS).

DISCUSSION AND CONCLUSIONS

Commonly, the formation of shock veins, including single and multiple veins, is attributed to shock-induced localized melting (Dodd and Jarosewich 1979; Dodd et al. 1982; Rubin 1985; Stöffler et al. 1991). The fine-grained matrix of both the early vein and the late vein in the complex veins of the Sixiangkou meteorite has similar compositions to the bulk chondrite, hence indicating the shock-induced in-situ melting of meteorite material. Abundant high-pressure minerals in the complex veins reflect shock-induced high-pressure and temperature excursions.

Columnar dendrites of garnet from the early veins and equant garnet from the late veins in Sixiangkou are indicative of crystallization from melt. Compositional analyses show that these garnets are relatively rich in CaO, Na_2O, and Al_2O_3, in comparison with low-Ca pyroxene and majorite transformed from pyroxene. This suggests that CaO, Na_2O, and Al_2O_3 in the shock-induced melt were partially scavenged by garnet. The fine-grained ringwoodite in the early vein could have simultaneously crystallized from melt together with dendrites of garnet, whereas the magnesiowüstite in the late vein had crystallized from melt together with equant garnet. Therefore, both assemblages of ringwoodite plus garnet in the early vein and magnesiowüstites plus garnet in the late vein could be liquidus phases crystallized at high pressures and temperatures.

A liquidus assemblage of high-pressure minerals has been found in the shock veins of numerous chondritic meteorites (Chen et al. 1996; Xie et al. 2001, 2004; Xie and Sharp 2004; Ohtani et al. 2004). The liquidus assemblages are important for the characterization of pressure and temperature conditions of melt crystallization (Chen et al. 1996; Xie et al. 2006). Commonly, the shock veins of a meteorite contain a

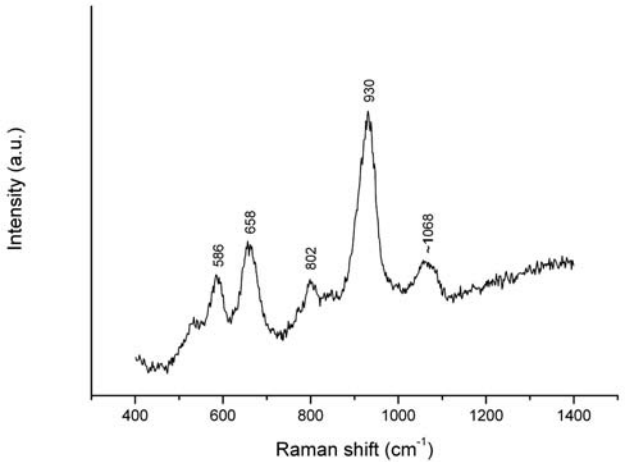

Fig. 6. Raman spectrum of garnet in the fine-grained matrix of the late vein.

type of liquidus assemblage. A recent investigation revealed two different liquidus assemblages in the simple shock vein of Tenham, in which garnet plus magnesiowüstite occurs in the center of vein, whereas ringwoodite, akimotoite, garnet, and vitrified silicate-perovskite occurs at in the edge of vein (Xie et al. 2006). It was explained that the two assemblages in the Tenham crystallized at the same pressure and different quench rates (Xie et al. 2006).

The distinct high-pressure assemblages in the early vein and the late vein of Sixiangkou demonstrate distinct pressure and temperature history. Based on the phase diagrams of the Allende meteorite (Agee et al. 1995), the liquidus phases of garnet plus magnesiowüstite crystallizes at pressures from 23 to 26 GPa and temperatures from 1950 to 2050 °C. The assemblage garnet plus ringwoodite crystallizes at 18 to 23 GPa and 1800 to 1950 °C (Fig. 7). It therefore appears that the late vein experienced higher pressures and temperatures

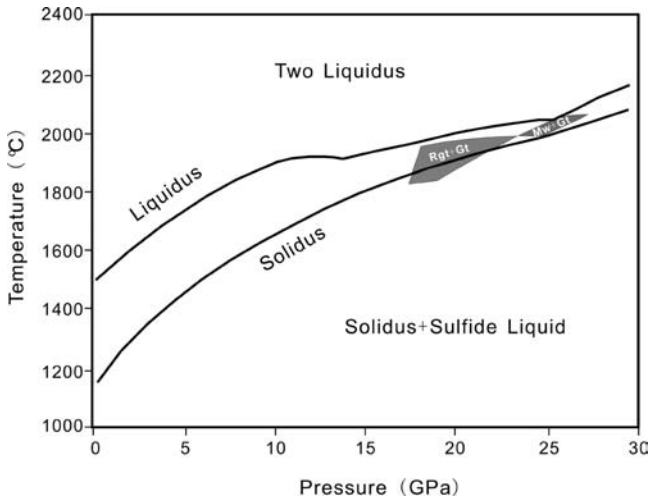

Fig. 7. Phase diagram for the Allende meteorite after Agee et al. (1995). Rgt = ringwoodite; Gt = garnet; Mw = magnesiowüstite.

than the early vein. Our observation also indicates that the early vein contains larger amount of coarse-grained aggregates of minerals and chondritic fragments than the late vein, whereas the late vein was nearly completely melted. This shows that the late vein achieved higher temperatures and underwent slower cooling than the early vein.

It has been suggested that the shock veins in meteorites are produced via a shearing melting mechanism triggered by the shock wave (Stöffler et al. 1991; Langenhorst and Poirier 2000). The multiple veins in the Sixiangkou meteorite could have been produced by two shearing/melting events, resulting in the formation of the early veins and the late vein, respectively. Since the late vein is predominantly located within the early vein, a still hot (or plastic) earlier vein could have hosted the later shock excursion event. The knife-sharp boundaries between the early and the late veins show that the late vein was produced as the early vein solidified, probably in subsolid state. Based on heat flow estimations, a time period of a few seconds is required to quench a shock melt vein of several millimeters thick from 2000 down to 600 °C (the bulk shock temperature of this meteorite), by which time ringwoodite, garnet, majorite, and lingunite could have crystallized on release of pressure (Chen et al. 2002). This shows that the interval forming the early vein and the late vein in the complex veins in Sixiangkou meteorite could have occurred within seconds of each other.

We speculate as to how two possibly contemporaneous events could have occurred in the Sixiangkou meteorite. Shock veins in meteorites are disequilibrium shock effects produced by local deviations of peak shock pressure from equilibrium pressure experienced by whole meteorite (Stöffler et al. 1988). The propagating shock wave may be reverberated on many interfaces causing a local stepwise increase or decrease of the shock pressure (Stöffler et al. 1991). A local increase or decrease of pressure may result in successive shearing within the shocked meteorite, thereby forming the complex veins. However, this scenario does not answer the question why the late vein experienced higher pressure and temperature than the early vein in an impact event. Alternatively, we may suggest that the meteorite may have experienced two impact events, with one following the other in a few seconds. If it is the case, the second impact producing the late vein had induced higher pressure and temperature than the first impact forming the early vein. This explanation may be coincident with shock excursion mechanics and the mineral assemblages found in the complex veins.

Acknowledgments—We thank John Spray, Allan Rubin, and Makoto Kimura for constructive comments and suggestions that have greatly approved quality of the paper. This project was supported by the National Natural Science Foundation of China (grants no. 40672035 to Ming Chen, no. 40772030 to Xiande Xie) and the Chinese Academy of Sciences (grant KJCX2-SW-N20).

Editorial Handling—Dr. John Spray

REFERENCES

Agee C. B., Li J., Shannon M. C., and Circone S. 1995. Pressure-temperature phase diagram for the Allende meteorite. *Journal of Geophysical Research* 100:17,725–17,740.

Chen M., Sharp T. G., El Goresy A., Wopenka B., and Xie X. 1996. The majorite-pyrope + magnesiowüstite assemblage: Constraints on the history of shock veins in chondrites. *Science* 271:1570–1573.

Chen M., Xie X., Wang D., and Wang S. 2002. Metal-troilite-magnetic assemblage in shock veins of Sixiangkou meteorite. *Geochimica et Cosmochimica Acta* 66:3143–3149.

Dodd R. T. and Jarosewich E. 1979. Incipient melting in and shock classification of L chondrites. *Earth and Planetary Science Letters* 44:335–340.

Dodd R. T., Jarosewich E., and Hill B. 1982. Petrogenesis of complex veins in the Chantonnay (L6f) chondrite. *Earth and Planetary Science Letters* 59:364–374.

Fredriksson K., De Carli P., and Aaramäe A. 1963. Shock-induced veins in chondrites. *Space Research* 3:974–983.

Gillet P., Chen M., Dubrovinsky L., and El Goresy A. 2000. Natural $NaAlSi_3O_8$-hollandite in the shocked Sixiangkou meteorite. *Science* 287:1633–1636.

Kimura M., Chen M., Yoshida Y., El Goresy A., and Ohtani E. 2003. Back-transformation of high-pressure phase in a shock melt vein of an H chondrite during atmospheric passage: Implications for the survival of high-pressure phases after decompression. *Earth and Planetary Science Letters* 217:141–150.

Langenhorst F. and Poirier J. P. 2000. "Eclogitic" minerals in a shocked basaltic meteorite. *Earth and Planetary Science Letters* 176:259–265.

McMillan P. and Akaogi M. 1987. Raman spectra of β–Mg_2SiO_4 (modified spinel) and γ–Mg_2SiO_4 (spinel). *American Mineralogist* 72:361–364.

Ohtani E., Kimura Y., Kimura M., Takata T., Kondo T., and Kubo T. 2004. Formation of high-pressure minerals in shocked L6 chondrite Yamato-791384: Constraints on shock conditions. *Earth and Planetary Science Letters* 227:505–515.

Rubin A. 1985. Impact melt products of chondritic material. *Reviews of Geophysics* 23:277–300.

Stöffler D., Bischoff A. Buchwald V., and Rubin A. E. 1988. Shock effects in meteorites. In *Meteorites and the early solar system*, edited by Kerridge J. F. and Matthews M. S. Tucson: The University of Arizona Press. pp. 165–202.

Stöffler D., Keil K., and Scott E. R. D. 1991. Shock metamorphism of ordinary chondritis. *Geochimica et Cosmochimica Acta* 55: 3845–3867.

Xie X., Chen M., and Wang D. 2001. Shock-related mineralogical features and P-T history of the Suizhou L6 chondrite. *European Journal of Mineralogy* 13:1177–1190.

Xie Z., Sharp T. G., and De Carli P. S. 2004. Shock pressures of impacts versus crystallization pressures of shock-induced melt veins of the chondrites (abstract #1308). 35th Lunar and Planetary Science Conference. CD-ROM.

Xie Z. and Sharp T. G. 2004. High-pressure phases in shock-induced melt veins of the Umbarger L6 chondrite: Constraints of shock pressure. *Meteoritics & Planetary Science* 39:2043–2054.

Xie Z., Sharp T. G., and De Carli P. S. 2006. High-pressure phases in shock-induced melt veins of the Tenham L6 chondrite: Constraints of shock pressure and duration. *Geochimica et Cosmochimica Acta* 70:504–515.